J Solid State Electrochem (2011) 15:2351–2359
DOI 10.1007/s10008-011-1401-0

ORIGINAL PAPER

Magnetic hybrid modified electrodes, based on magnetite nanoparticle containing polyaniline and poly (3,4-ethylenedioxythiophene)

Csaba Janáky · Attila Kormányos · Csaba Visy

Received: 29 March 2011 / Revised: 4 April 2011 / Accepted: 4 April 2011 / Published online: 4 May 2011

Abstract In this paper, we report on the direct electrodeposition of magnetic hybrids based on magnetite nanoparticle containing poly(3,4-ethylenedioxythiophene) (PEDOT) and polyaniline (PANI) in the presence of magnetite and the special conducting electrolyte, potassium tetraoxalate. The optimal electropolymerization processes (monitored by scanning electron microscopy) were performed potentiostatically, and the incorporation of the iron oxide into the polymeric film was demonstrated by Diffuse Reflectance UV-Visible Spectroscopy (DR-UV–vis) and transmission electron microscopic measurements. Electrochemical quartz crystal nanobalance proved that both the neat PEDOT and the PEDOT/magnetite hybrid show anion exchange behaviour. Cyclic voltammetric features of the polymers and their hybrids exhibited an enhanced redox capacity of the composites. The difference in the effect of the scanning rate on this capacity increase in the two cases could be interpreted by the assumption that the presence of magnetite manifests dominantly in the enhanced intrinsic electroactivity of PANI, while in the case of the PEDOT composite, the extra charge is more connected to the charge surplus originating from the redox activity of the nanoparticles.

Keywords Poly(3,4-ethylenedioxythiophene) · Polyaniline · Magnetite · Nanocomposite · Supercapacitor · EMI shielding

Introduction

Conjugated polymer based hybrids, containing inorganic nanoparticles form one of the most extensively studied class of new materials. Polyaniline (PANI) and poly(3,4-ethylenedioxythiophene) (PEDOT) are in the focus of research and development due to their favourable features which have been exploited in a wide range of applications from corrosion protection to electrocatalysis [1–5].

Nanocomposites of different metal oxides and conducting polymers give unique combinations of advantageous properties of the inorganic nanoparticles and the conducting organic matrix [6, 7]. Beyond the most frequently applied polypyrrole, various inorganic oxides such as ferrites [8], titanium dioxide [9], vanadium pentoxide [10], ruthenium dioxide [11], etc., have been successfully incorporated into PEDOT and PANI films. Since the embedded nanoparticle can enhance the intrinsic activity of the polymer, such hybrid modified electrodes can be even more effectively utilized—among others—in microwave absorbers [12], electrocatalysis [13], sensors [14] and supercapacitors [15, 16]. Incorporation of different ferrites and especially iron oxides into polyaniline is particularly promising for EMI shielding and supercapacitor applications. Several studies have been published on polyaniline/magnetite hybrids [17–19], where different methods have been successfully applied for the preparation of such materials.

Iron oxide-containing PEDOT nanocomposites [20–22] have also been synthesized by applying either simple or

The article is dedicated to the 65th birthday of George Inzelt, whose pioneering work has contributed a lot to the general knowledge in the field of the elucidation of ionic and molecular movements during the redox switching process of conjugated polymer films.

C. Janáky · A. Kormányos · C. Visy (✉)
Department of Physical Chemistry and Materials Science,
University of Szeged,
Aradi V. Sq. 1,
Szeged 6720, Hungary
e-mail: visy@chem.u-szeged.hu

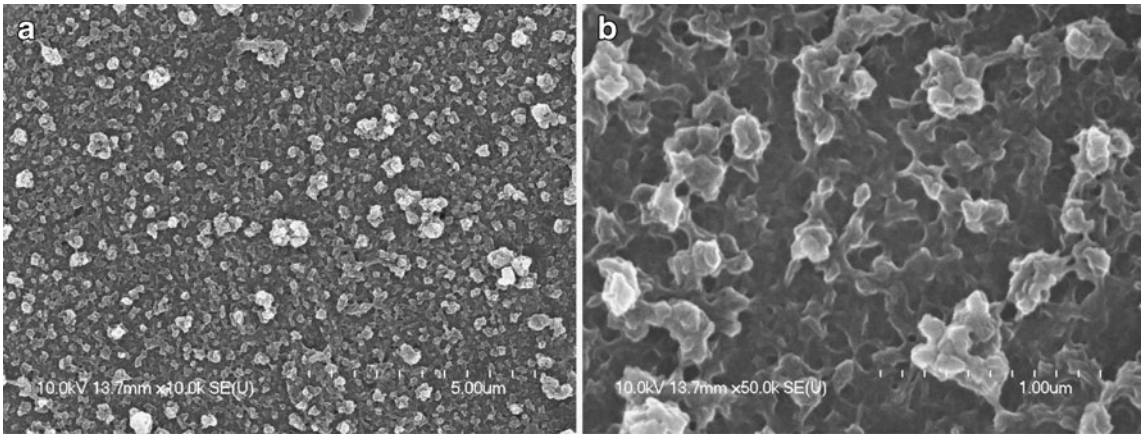

Fig. 1 SEM images of the PEDOT film, electrosynthesized on Pt electrode, at E=1.1 V, in aqueous PTO (0.05 M) solution with a charge density of 120 mC cm^{-2}. **a** ×10,000 magnification. **b** ×50,000 magnification

more sophisticated preparative methods. Direct electrodeposition of these magnetite containing hybrid materials can be very advantageous from the point of utilization since the composite can be prompted as a thin layer on the electrode surface. During recent years, two synthetic procedures have been developed to enrich iron oxide particles in the polymeric film, in which—beyond the week physisorption—chemical interactions between either the Fe_3O_4 nanoparticles and the monomer [23], or the nanoparticles and the conducting electrolyte [24–27] have been exploited. This latter is an easy, aqueous solution synthesis, where the inclusion of magnetite nanoparticles is connected to their surface modification—due to their reaction with the potassium tetraoxalate-supporting electrolyte—and takes place during the anodic polymerization as a part of the charge compensation (doping by the negatively charged nanoparticles). By this method, the magnetite content could be increased up to 27 m/m% [27].

In this work, our goal was to apply the abovementioned procedure to prepare novel hybrid materials. Here, we report on the electrochemical synthesis and characterization of PEDOT/magnetite hybrids and PANI/magnetite modified electrodes, by adapting the synthetic procedure, used earlier for the electrosynthesis of polypyrrole/magnetite layers. This work is original since according to the best of our knowledge, this is the first time, when superparamagnetic iron oxide-containing PEDOT- and PANI-based composite layers have been prepared through a direct electrodeposition process.

This procedure may foster the further research towards the application of these hybrid materials both as supercapacitors and in electromagnetic shielding since they are

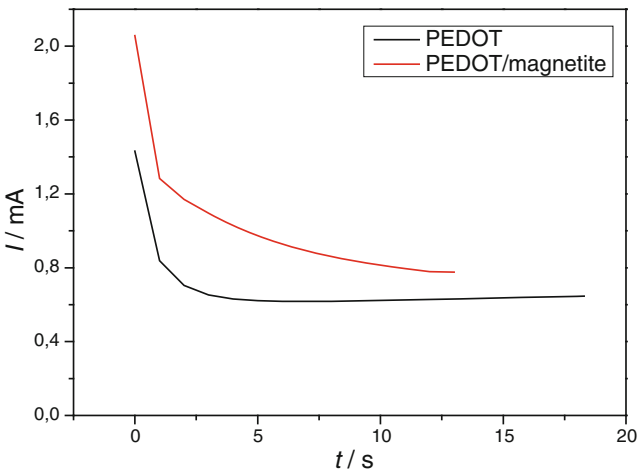

Fig. 2 Chronoamperometric polymerization curves of the PEDOT and PEDOT/magnetite layers at E=1.1 V in aqueous PTO (0.05 M) solution with a charge density of 60 mC cm^{-2}

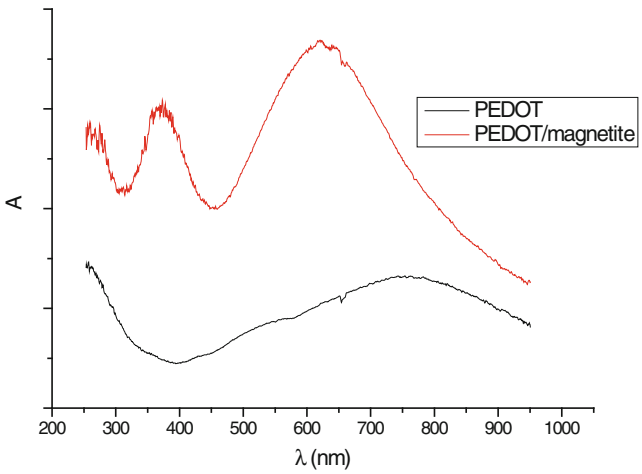

Fig. 3 DR-UV–vis spectra of the neat PEDOT-, and the PEDOT/magnetite layers deposited onto Pt electrode as in Fig. 1

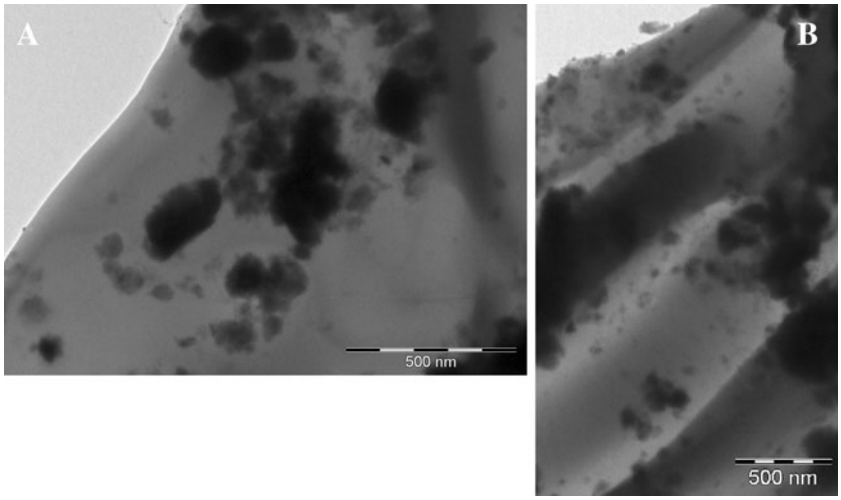

Fig. 4 Transmission electron microscopic images of the PEDOT/magnetite hybrid at **a** ×25,000 and **b** ×10,000 magnification as in Fig. 3

directly prepared on the electrode surface; thus, no further processing step is needed before utilization.

Experimental

Analytical grade 3,4-ethylene-dioxythiophene (EDOT) was the kind donation of Bayer AG, while aniline and potassium tetraoxalate dihydrate (PTO, $KH_3(C_2O_4)_2 \times 2H_2O$) were purchased from Sigma-Aldrich. The monomers were freshly distilled before use. Magnetite (Fe_3O_4) nanoparticles were synthesized by alkaline hydrolysis of iron(II) and iron(III) salts ($FeCl_2 \times 4H_2O$ and $FeCl_3 \times 6H_2O$, Sigma-Aldrich) [28]. The concentrated solutions of iron(II) and iron(III) salts were mixed in the ratio of 1.1–2 and filtered into distilled water using a 0.2-μm microfiltre. NaOH solution was added in 10% excess to the double diluted iron salt solution in two portions under rigorous stirring. The formed black suspension was stirred further for some minutes and then transferred into a larger amount of distilled water. The suspension was washed several times with water and then acidified with HCl solution down to pH~2. Finally, it was washed with water until peptization and dialyzed against 0.001 M HCl. The characterization of the particles prepared in this way was reported elsewhere [29]. The synthesis resulted magnetite nanoparticles with an average size around 12 nm.

The polymerizations were carried out from solutions containing 0.05 M PTO in deionized water in all cases, while the concentration of the monomer was 0.01 and 0.05 M in the case of EDOT and aniline, respectively. The amount of magnetite particles was 10 $g dm^{-3}$. Poly (3,4-ethylenedioxythiophene) (PEDOT) and PEDOT/magnetite composite thin films were deposited potentiostatically at a potential of $E=1.1$ V onto the platinum working electrode ($A=1.00$ cm^2), with a charge density of 120 mC cm^{-2}. In the case of the measurements with electrochemical quartz crystal nanobalance (EQCN), charge density was limited to 60 mC cm^{-2}, in order to avoid viscoelastic effects [30]. As for the PANI and PANI–magnetite hybrids, they were deposited potentiostatically at $E=1.1$ V potential onto gold working electrode ($A=1.00$ cm^2), with a charge density of 40 mC cm^{-2}. For further voltammetric studies, the solution was changed after the polymerization to a 0.05 M PTO solution in water.

The electrochemical measurements were performed on a PGSTAT 302 (Autolab) instrument, in a classical three electrode electrochemical cell. The working electrode was a platinum or gold electrode with a size of $A=1.00$ cm^2. Ag/AgCl/3 M NaCl reference electrode having a potential 0.200 V vs. SHE was used. All the potential values in the paper are given with respect of the silver/silver chloride electrode. The Autolab Electrochemical Quartz Crystal Nanobalance (EQCN) module was used for the nanogravimetric measurements, applying gold-coated quartz crystal electrode ($f_0=6$ MHz, $A=0.361$ cm^2). The EQCN system was calibrated by electrochemical lead deposition using the standard procedure, and the value of 5.04 ng Hz^{-1} coefficient was obtained for the crystal $f_0=6$ MHz. Cyclic voltammograms of the thin films were registered at five different sweep rates (5, 10, 25, 50 and 100 mV s^{-1}). All electrochemical measurements were carried out in nitrogen atmosphere, where nitrogen gas was bubbled into the solutions for 30 min before the experiments.

Transmission electron microscopic (TEM) investigation of the PEDOT/magnetite composite layer—after peeling it off from the electrode—was performed using a Philips CM 10-type instrument, operating at an acceleration voltage of 100 kV. The morphology of the polymeric films was studied using a Hitachi S-4700 field emission scanning electron microscope. UV–visible diffuse reflectance spectra were recorded with an AvaSpec-2048 spectrometer from 180 to 800 nm, where an AvaLight-DH-S light source was utilized.

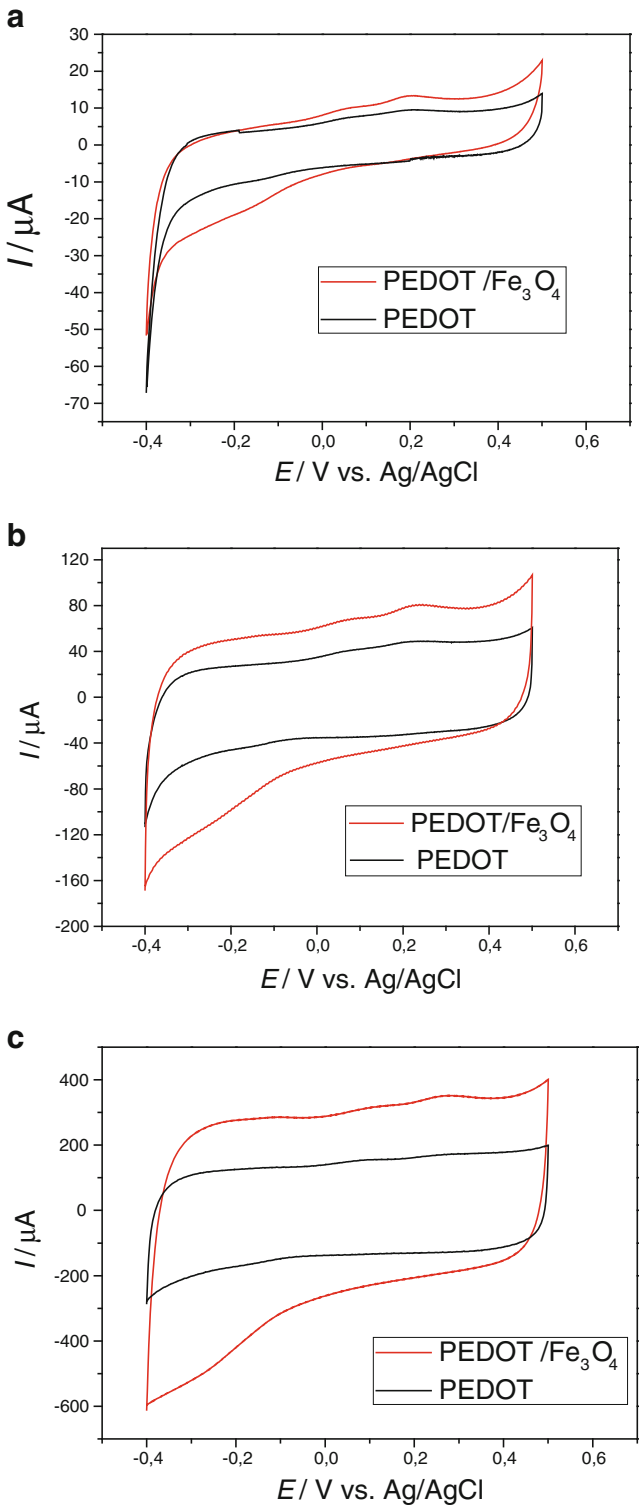

Fig. 5 Cyclic voltammograms of the PEDOT and PEDOT/magnetite layers at **a** 5-mV s^{-1}, **b** 25-mV s^{-1} and **c** 100-mV s^{-1} scan rate in 0.05 M PTO solution

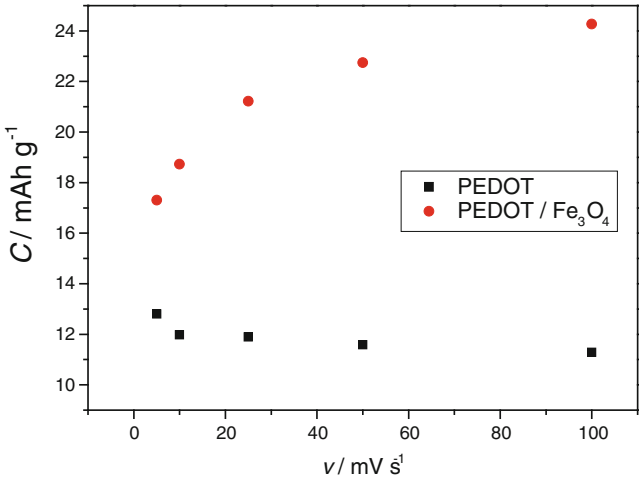

Fig. 6 Sweep rate dependence of the charge capacity of the PEDOT and the PEDOT/magnetite layers

Results and discussions

Synthesis of PEDOT layers

As the first step we investigated the polymerization of EDOT in the presence of the special conducting electrolyte, aqueous potassium-tetraoxalate. This was indeed important, since – according to the best of our knowledge – PEDOT has never been prepared in such a solution. After the thorough optimization process, we selected potentiostatic procedure, at a potential of E=1.1 V. By this method we were able to deposit the polymeric film both on platinum and gold working electrode. According to the scanning electron microscopy (SEM) pictures taken at different magnifications, the synthesized layers show the typical morphology obtained previously for the polymers of thiophene-derivatives, although they are quite smooth compared to PEDOT films prepared in the presence of other dopants [31]. Moreover, Fig. 1 demonstrates that the growth of the polymer is continuous on the electrode, it looks rather uniform even at large magnifications, although the morphology of the polymer is rather porous.

Synthesis of PEDOT/magnetite layers

After optimizing the polymerization conditions for the neat PEDOT, we synthesized the PEDOT/magnetite hybrid layers under totally identical conditions, but in the presence of magnetite nanoparticles. The comparison of the polymerization curves in Fig. 2 shows that in the presence of magnetite, higher current densities can be obtained. It may suggest that the deposition is faster at the same oxidation potential, which in fact may be related to the better/faster doping by the surface modified, negatively charged nanoparticles. Otherwise, the shape of the curves is similar, indicating that the

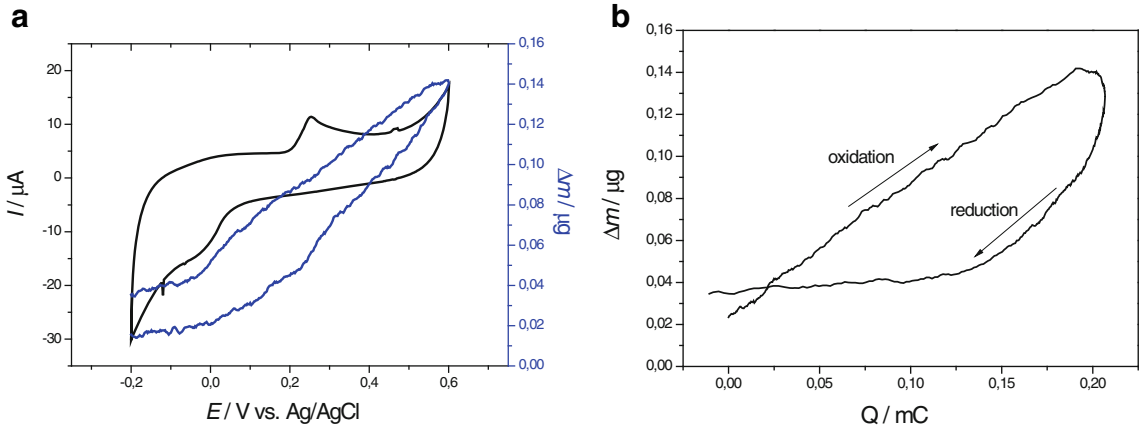

Fig. 7 **a** Cyclic voltammogram of PEDOT, recorded at 25-mV s^{-1} sweep rate in 0.05 M PTO in water together with the mass change recorded by EQCN. **b** Δm–Q curve calculated from data presented in **a**

presence of the iron oxide does not disturb the polymerization process. This is in agreement with our previous experience with PPy/magnetite, where the polymerization occurred at lower potentials during the galvanostatic electrosynthesis [27].

In order to prove the incorporation of the magnetite into the polymeric film, we performed—as a first step—Diffuse Reflectance UV-Visible Spectroscopy (DR-UV–vis) measurements. With this technique we can obtain the UV–vis spectra of materials deposited on non-transparent substrates (Pt electrodes in our case). Figure 3 contains typical diffuse reflectance UV-Visible spectra of the neat PEDOT and the corresponding PEDOT/Fe_3O_4 hybrid. One can see that the neat PEDOT has only one broad absorption band (around 700–800 nm), which can be connected to the excitation of the conducting polymer. For the hybrid sample, two characteristic light absorption bands can be observed. One corresponds to the band gap of Fe_3O_4 (380 nm) [32], while the other originates from the presence of PEDOT (620 nm) [33]. By comparing the spectrum for PEDOT/Fe_3O_4 with that for PEDOT electrodeposited on Pt, the second broad absorption band can be readily assigned to the conjugated polymer, while the shift in the position of the maximum can be related to the difference in the oxidation level of the polymer.

To gain further evidence for the presence of iron oxide particles in the PEDOT layer, we peeled of the hybrid film from the electrode and took TEM pictures. When we studied the thin layer of the composite—beyond the appearance of the grey background of the polymeric film—we could observe the randomly distributed dark spots originating from the encapsulated iron oxide particles. Fig. 4a, b proves the incorporation of magnetite into the polymeric layer, although not the primary sized particles, but their aggregates can be dominantly detected. This observation is not surprising, since no surfactant was used during the synthesis. The presence of any stabilizing agent could have hindered the surface modification of the nanoparticles through the reaction with the conducting electrolyte [27].

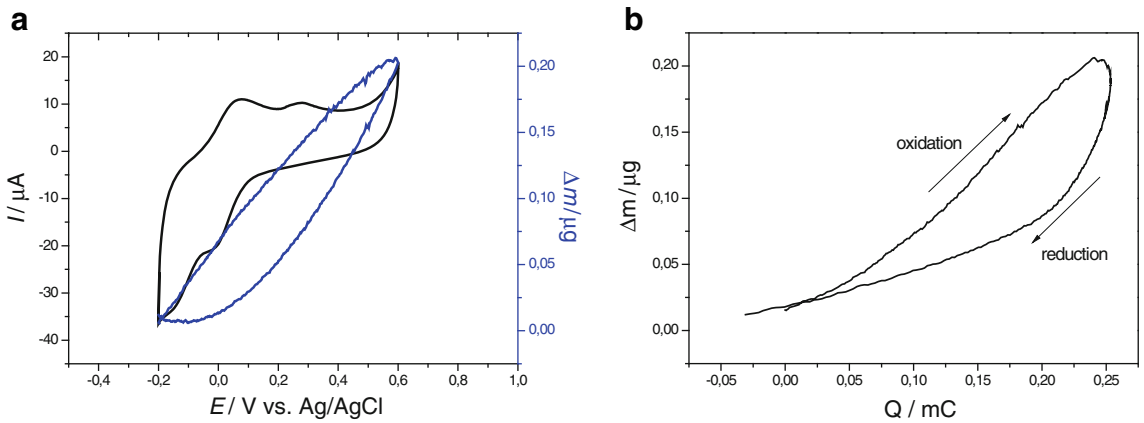

Fig. 8 **a** Cyclic voltammogram of the PEDOT/magnetite hybrid, recorded at 25-mV s^{-1} sweep rate in 0.05 M PTO in water together with the mass change recorded by EQCN. **b** Δm–Q curve calculated from data presented in **a**

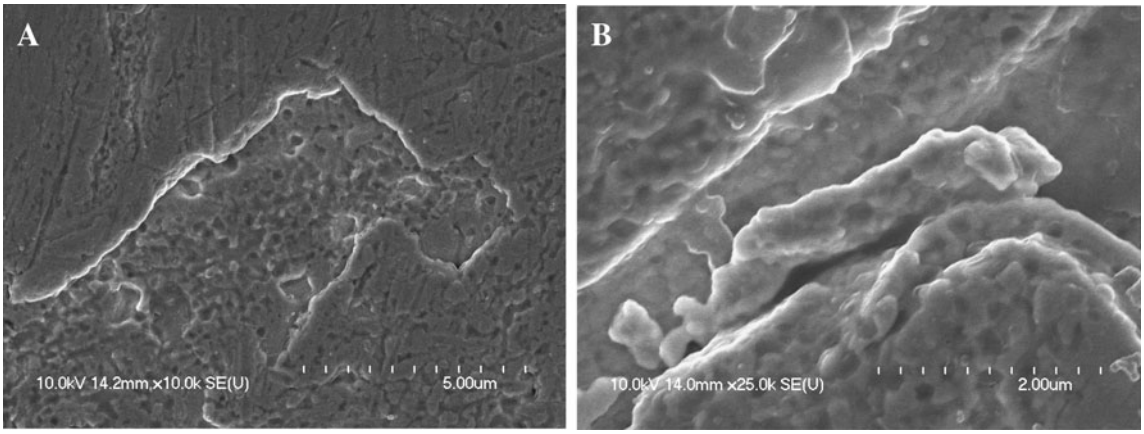

Fig. 9 SEM image of a PANI film, electrosynthesized on Au electrode with a charge density of 40 mC cm^{-2}, at **a** ×10,000 and **b** ×25,000 magnification

Comparative electrochemical studies

In order to compare the neat PEDOT and PEDOT/magnetite layers, their electrochemical behaviour was studied. In Fig. 5a–c, representative voltammograms of the two layers (both synthesized by 120 mC cm^{-2}) at three selected scan rates (5, 25 and 100 mV s^{-1}) are shown, where the shape of the curves reflects on the reversible electroactivity of both the polymer and the hybrid. The cycling was started from the negative end of the potential window, and the curves have been recorded in N_2 atmosphere. The curves obtained for PEDOT itself show a relatively weak redox behaviour, assumingly due to the poor quality of the film originating from the dopant. This behaviour has been already reported for polypyrrole films, prepared in the presence of oxalate ions [34]. As for the nanocomposite layers, the more complex redox activity and the additional redox couple can be revealed at all sweep rates. It is also important to emphasize that the pattern of the curves is gradually changing with the increasing scan rate; namely, the capacitive behaviour of the films becomes more and more recognizable. It is also visible that the magnetite-containing layer has an enhanced electroactivity, resulting in larger current densities in the whole potential range. This qualitative picture can be quantified, if we present the charge capacity of the films as the function of the sweep rate, shown in Fig. 6. For the sake of comparability, the specific charges are plotted for the two layers, where the mass was estimated, based on separate EQCN measurements, shown later. The first obvious difference is the significantly larger charge capacities of the nanocomposite layer, compared to the neat PEDOT, at all sweep rates. The more careful investigation of the curves reveals a difference also in the trend of the capacitance values, namely an increase for the hybrid and a decrease for the neat polymer in function of the scan rate. This may suggest that the contribution of the incorporated nanoparticles to the electroactivity of the hybrid material involves not only the enhancement of the redox activity of the PEDOT itself (through more effective doping) but also the extra electroactivity of the encapsulated particles.

In order to get more information about the electrochemical behaviour of the neat PEDOT and the hybrid, we carried out EQCN measurements during repetitive cycles, run between the reduced and oxidized forms. As it was comprehensively demonstrated by Inzelt et al., electrochemical nanogravimetry is a widely applicable method to investigate the mass changes connected to the doping–dedoping processes of conjugated polymers and their composites [35–37].

First, we present the mass changes, simultaneously recorded with the cyclic voltammograms. As Figs. 7a and 8a document, the mass change curves reflect on the anion-

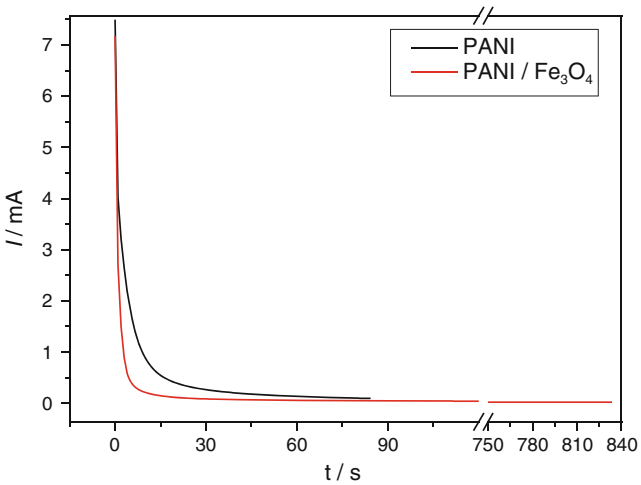

Fig. 10 Chronoamperometric polymerization curves of the PANI and PANI/magnetite layers at E=1.1 V in aqueous PTO (0.05 M) solution with a charge density of 40 mC cm^{-2}

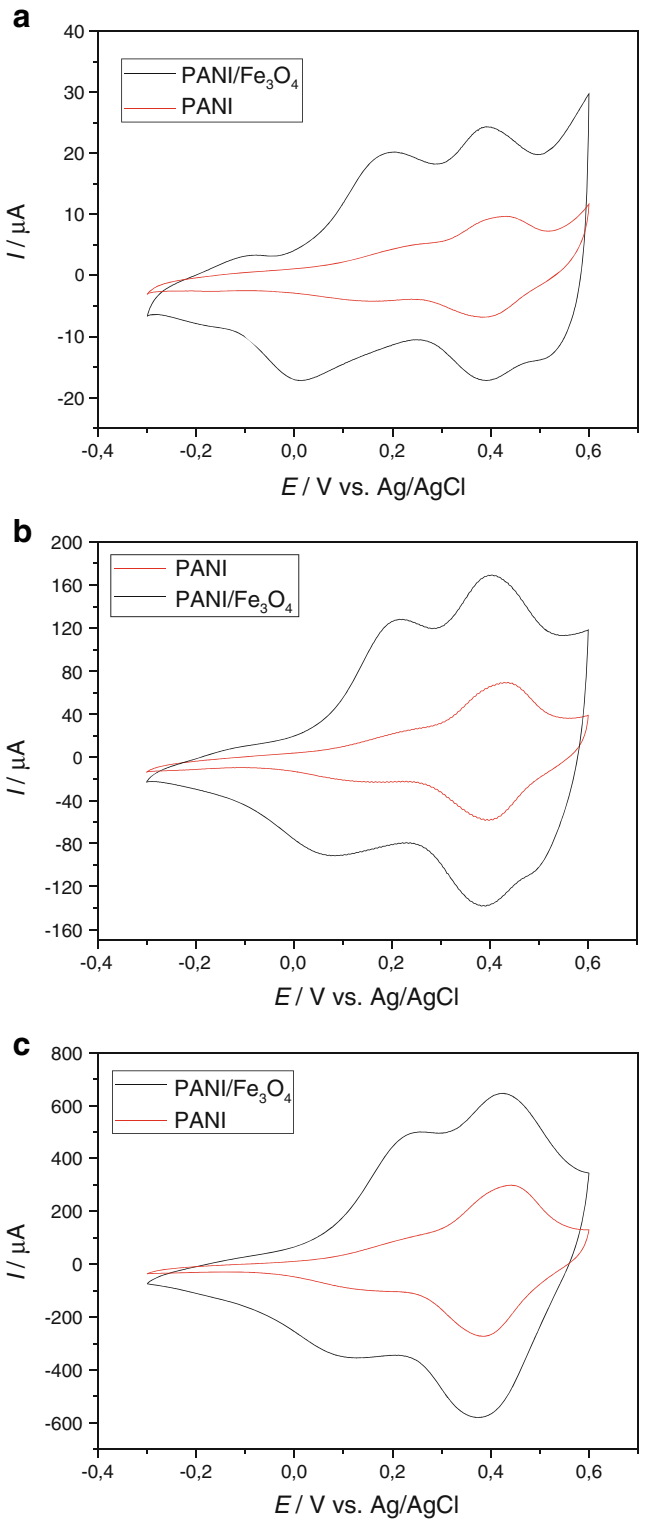

Fig. 11 Cyclic voltammograms of the PANI and PANI/magnetite layers at **a** 5-mV s^{-1}, **b** 25-mV s^{-1} and **c** 100-mV s^{-1} scan rate in 0.05 M PTO solution

exchanging property of both samples, since the mass of the films increases monotonously during the oxidation and decreases back to the original value during the reduction. The extra redox transition connected to the $Fe^{2+/}Fe^{3+}$ redox coupled can be undoubtedly seen in Fig. 8a which is even more expressed in this case, due to the inevitable presence of oxygen in the applied EQCN cell.

In order to quantify the mass changes, we transformed EQCN data into Δm–Q curves, which are presented in Figs. 7b and 8b. One can readily see the complexity of the doping/dedoping process, both for the neat polymer and the composite. While the oxidative branch exhibits a more or less linear character, indicating a stationary process, the mass decrease can be divided into two sections.

When we calculated the virtual molar mass of the incorporating particles from the slope of the curve, registered during the oxidation PEDOT, we obtained an almost constant, but definitely smaller value than that of the H-oxalate anion (89 $gmol^{-1}$). In contrast, in the case of the hybrid, this value decreased monotonously but in the range close to the value of a value of 89 $gmol^{-1}$ (~82 $gmol^{-1}$, at 25 mV s^{-1}). Since it is rather improbable that the moving anion depends on the scan rate, we may assume that with increasing sweep rate, the ratio between capacitive and Faradaic-type charges is also increasing, in agreement with our previous explanation connected to Fig. 6.

Synthesis of polyaniline and polyaniline/magnetite layers

Similar to PEDOT, first, we studied the electropolymerization of aniline in the presence of potassium tetraoxalate. Oxalic acid has been previously used as electrolyte during the electrodeposition of PANI onto various substrates [38]. After trying various procedures, we found the potentiostatic electrodeposition onto platinum electrode, at constant E=1.1 V potential to be the most convenient method. According to the SEM pictures, we were able to synthesize relatively thin (400–500 nm), homogenous layers, which have very smooth surface. In addition, in Fig. 9, some islands can be seen, where only a thinner polymeric film covers the Pt substrate, demonstrating that the growth of the polymer is not uniform on the electrode.

In Fig. 10, we compare the chronoamperometric polymerization curves of neat PANI and the iron oxide-containing hybrid, carried out under totally identical conditions. One can recognize the similar pattern of the curves, although a significantly longer time is needed for the hybrid to accomplish the 40 mC cm^{-2} polymerization charge density. This is different from the trend observed for PEDOT and PPy earlier, which might be connected to the fact that PANI should be prepared in strong acidic media. Aqueous PTO ensures the necessarily small pH value for the successful polymerization; however, when magnetite is present, its reaction with the conducting electrolyte results in an increase in the pH, which, in turn, inhibits the deposition of a well-conducting film.

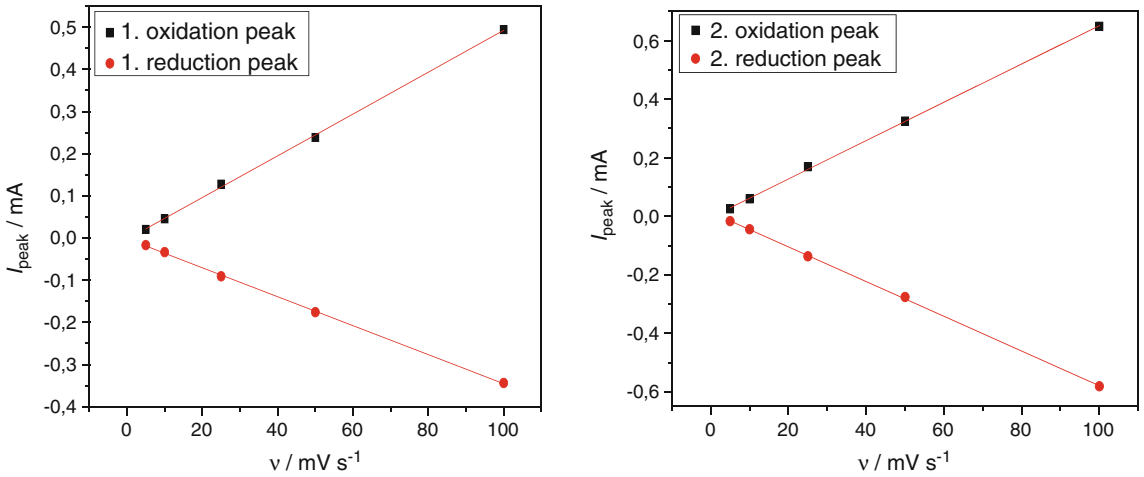

Fig. 12 Analysis of the anodic and cathodic peak currents vs. scan rate data from Fig. 11

Redox transformation of the PANI and the PANI/magnetite hybrid has been studied by cyclic voltammetry at five different sweep rates between 5 and 100 mV s^{-1} (Fig. 11). Although the well-known quasi-reversible redox activity—typical for conjugated polymers—is visible in both cases, some significant distinction can be made. First of all, the shape of the voltammograms is dissimilar in two aspects: (1) the hybrid exhibits significantly larger electroactivity in the whole potential range (from −0.3 to 0.6 V), and (2) in the case of the composite one—at lower sweep rates two—new redox couple becomes more expressed at E_{ox}≈0.2 V and at E_{red}≈0.05 V.

Closer inspection of the redox activity of the hybrid was carried out by comparing the peak currents obtained at different scan rates. Figure 12 shows that the peak currents of both redox couples are directly proportional to the sweep rate, and their position is almost constant (for the anodic range), indicating that we observe the redox transformation of a surface-related material, and there is no mass transport limitation under the applied circumstances.

We quantified the difference in the charge capacity of the layers by comparing the total charge flown during the voltammetric curves at the different sweep rates. Opposite to PEDOT, both curves show the same tendency, namely that after an increase at small sweep rates, the charge values are slightly decreasing. The difference in the values, shown in Fig. 13a, is striking: approximately three times larger charge capacities can be observed for the PANI/magnetite hybrid material, compared to the neat polyaniline. These results are presented in Fig. 13b, where the ratio is almost independent of the scan rate. This observation is coherent with the character of the additional electroactivity described in connection with Fig. 11, since the three times larger charge capacity can be dominantly related to the improved

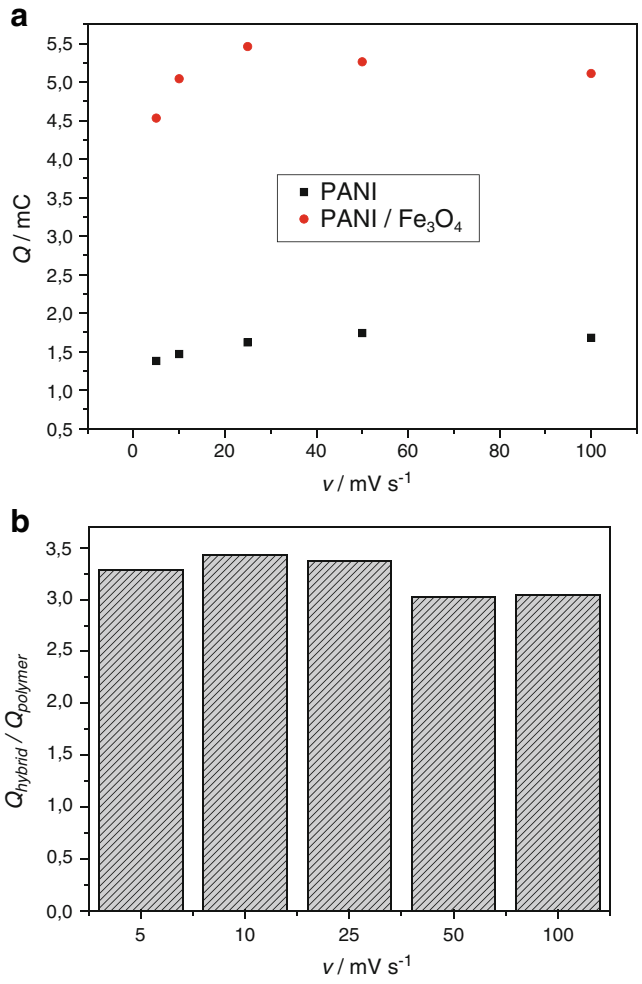

Fig. 13 Sweep rate dependence of the charge capacity of the PANI and the PANI/magnetite layers (**a**), and their ratio at the presented five scan rates (**b**)

redox behaviour of PANI itself. This may be the consequence of the modification of the polymer, manifesting also in the more characteristic shape of the voltammograms.

Conclusions

As a first step, we demonstrated that—after thorough optimization—both monomers can be electropolymerized in the presence of the used special conducting electrolyte, potassium tetraoxalate. Utilizing this procedure, we presented its feasibility for the synthesis of both PEDOT- and PANI-based hybrids. The composite formation is based on the participation of the surface-modified iron oxide nanoparticles in the charge compensation during the polymerization, reported earlier for polypyrrole/magnetite nanocomposites.

The incorporation of the magnetite was proved by DR-UV–Vis spectra, where the absorption band characteristic for magnetite was superimposed to that of PEDOT. Further direct evidence was gained from TEM images, where beyond the background of the polymeric film, the randomly distributed, partially aggregated iron oxide particles could be detected. According to cyclic voltammetric measurements, the encapsulation of the nanoparticles resulted in an enhanced redox activity in the whole potential range. From the opposite effect of the sweep rate on the redox capacities of the neat PEDOT and the composite, we may conclude that the electroactivity of the incorporated iron oxide contributed also directly to the charge increase. Electrochemical nanogravimetric data gave evidence for the anion exchanging property of both PEDOT and its magnetic hybrid.

Investigation of PANI and PANI/magnetite films demonstrated the improved electroactivity of the hybrid compared to the identically synthesized neat polymer. However, the similarity in the sweep rate dependence of the charge capacities (the almost constant ratio, which is 3) suggests that here the effect of the presence of magnetite manifests dominantly in the enhanced intrinsic electroactivity of the conjugated polymer.

Based on the increased charge capacity of magnetite containing polymers, it is strongly believed that these models may serve as base further studies towards the development of supercapacitors. These composites are promising also as EMI shielding materials; thus, investigation also in this direction is in progress.

Acknowledgements Financial support from the Hungarian National Research Fund (OTKA no. K72989) and the support from the National Development Agency through the project TÁMOP-4.2.1/B-09/1/KONV-2010-0005 are gratefully acknowledged.

References

1. Inzelt G (2008) Conducting polymers, a new era in electrochemistry. Monographs in electrochemistry. Springer, Leipzig
2. Wang YY, Jing XL (2005) Polym Advan Technol 16:344
3. Tallman DE, Spinks G, Dominis A, Wallace GG (2002) J Solid State Electrochem 6:73
4. Zhou HH, Chen H, Luo SL, Lu GW, Wei WZ, Kuang YF (2005) J Solid State Electrochem 9:574
5. Malinauskas A (1999) Synth Met 107:75
6. Gomez-Romero P (2001) Adv Mater 13:163
7. Rajeshwar K, de Tacconi NR, Chenthamarakshan CR (2001) Chem Mater 13:2765
8. Gangopadhyay R, De A (2000) Chem Mater 12:608
9. Janaky C, Bencsik G, Racz A, Visy C, de Tacconi NR, Chanmanee W, Rajeshwar K (2010) Langmuir 26:13697
10. Gomez-Romero P, Ayyad O, Suárez-Guevara J, Muñoz-Rojas D (2010) J Solid State Electrochem 14:1939
11. Sopčić S, Kraljić Roković M, Mandić Z, Inzelt G (2010) J Solid State Electrochem 14:2021
12. Ohlan A, Singh K, Chandra A, Dhawan SK (2008) J Appl Polymer Sci 108:2218
13. de Souza FG, Marins JA, Pinto JC, de Oliveira GE, Rodrigues CM, Lima LMTR (2010) J Mater Sci 45:5012
14. Tai HL, Jiang YD, Xie GZ, Yu JS (2010) J Mater Sci Technol 26:605
15. Szymanska D, Rutkowska IA, Adamczyk L, Zoladek S, Kulesza PJ (2010) J Solid State Electrochem 14:2049
16. Kwon CW, Murugan AV, Campet G, Portier J, Kale BB, Vijaymohanan K, Choy JH (2002) Electrochem Commun 4:384
17. Umare SS, Shambharkar BH, Ningthoujam RS (2010) Synth Met 160:1815
18. Radhakrishnan S, Prakash S, Rao CRK, Vijayan M (2009) Electrochem Solid St 12:A84
19. Wang ZZ, Bi H, Liu J, Sun T, Wu XL (2008) J Magn Magn Mater 320:2132
20. Reddy KR, Park W, Sin BC, Noh J, Lee Y (2009) J Colloid Interf Sci 335:34
21. Singh K, Ohlan A, Saini P, Dhawan SK (2008) Polym AdvanTechnol 19:229
22. Shin S, Yoon H, Jang J (2008) Catal Commun 10:178
23. Janaky C, Visy C, Berkesi O et al (2009) J Phys Chem C 113:1352
24. Bidan G, Jarjayes O, Fruchart F et al (1994) Adv Mater 6:152
25. Garcia B, Lamzoudi A, Deslouis C et al (2002) J Electrochem Soc 149:B560
26. Pailleret A, Hien NTL, Deslouis C (2007) J Solid State Electrochem 11:1013
27. Janaky C, Endrodi B, Berkesi O, Visy C (2010) J Phys Chem C 114:19338
28. Illés E, Tombácz E (2003) Colloids Surf A 230:99
29. Illés E, Tombácz E (2006) J Colloid Interf Sci 295:115
30. Skompska M, Jackson A, Hillman AR (2000) PCCP 20:4748
31. Wang XJ, Sjoberg-Eerola P, Eriksson JE et al (2010) Synth Met 160:1373
32. Cornell RM, Schwertmann U (1996) The iron oxides, VCH, Weinheim, p. 573. and p. 207.
33. Łapkowski M, Pron A (2000) Synth Met 110:79
34. Janaky C, Endrodi B, Hajdu A, Visy C (2010) J Solid State Electrochem 14:339
35. Inzelt G (1990) J Electroanal Chem 287:171
36. Inzelt G, Kertesz V, Nyback AS (1999) J Solid State Electrochem 3:251
37. Inzelt G, Roka A (2008) Electrochim Acta 53:3932
38. Camalet JL, Lacroix JC, Aeiyach S, Chane-Ching K, Lacaze PC (1998) Synth Met 93:133